JOURNAL OF GEOPHYSICAL RESEARCH, VOL. 114, C07002, doi:10.1029/2008JC004904, 2009

Climatic circulation in the Gulf of Trieste (northern Adriatic)

V. Malačič[1] and B. Petelin[1]

Received 7 May 2008; revised 15 March 2009; accepted 3 April 2009; published 2 July 2009.

[1] The climatic circulation of the Gulf of Trieste, which is a shallow semienclosed basin in the closed northeastern end of the northern Adriatic, is studied with a numerical model. In all seasons there is a general inflow into the Gulf of Trieste at its lower, deeper part. This inflow makes a cyclonic turn centered in the southern part during average winter conditions. This turn is enhanced during spring and closes in an elongated cyclonic gyre during average summer conditions. In spring and summer, the cyclonic gyre is coupled with an anticyclonic gyre near the closed eastern part of the gulf. A "dome"-like density profile across the gulf's axis in the inner part of the gulf above the bottom appears with this circulation during spring and summer. In climatic autumn there is a smaller anticyclonic gyre on its southern side. Near the sea surface there is an outflow during winter, which is driven by the dominant "bora" wind blowing along the gulf's axis. This outflow, however, is detached from the southern coastline to the right, and crosses the gulf diagonally, merging with the belt of freshwater outflow along the northern coastline. This is shown to be a consequence of the balance between the pressure gradient force caused by elevation piled up in the direction out of the gulf, the Coriolis force, and vertical friction between layers near the sea surface. During the stratified season the surface of the gulf is occupied by an anticyclonic gyre due to the inertial plume of the Isonzo River.

Citation: Malačič, V., and B. Petelin (2009), Climatic circulation in the Gulf of Trieste (northern Adriatic), *J. Geophys. Res.*, *114*, C07002, doi:10.1029/2008JC004904.

1. Introduction

[2] The first climatic circulation model of the Adriatic Sea was the Adriatic Intermediate Model (AIM), with a horizontal resolution of 5 km [*Zavatarelli et al.*, 2002]. Later, the Northern Adriatic Shelf Model (NASM) was developed, which had a horizontal resolution of 1.5 km and was nested into the AIM model [*Zavatarelli and Pinardi*, 2003].

[3] The AIM demonstrated that, over the northern Adriatic area during winter, a typical cyclonic circulation in the surface layer dominates [*Zavatarelli and Pinardi*, 2003], in which the rim current near the coastline extends about 10–20 miles offshore, while the NASM gave a more complex circulation pattern. From the point of view of the exchange of water mass of the Gulf of Trieste with the rest of the northern Adriatic, the AIM shows that the water mass at the surface of the gulf merges with the northward current coming along the Istria peninsula and leaves the gulf along the northern, Italian coastline, while the NASM predicts that the surface water mass simply exits the gulf along its axis.

[4] During summer, the AIM drives the surface current northward along the peninsula of Istria, as in winter, it merely reproduces the cyclonic circulation pattern. The surface circulation predicted by NASM deviates abruptly from that of the AIM, since the surface current is flowing in the opposite direction along the peninsula of Istria. NASM also shows that there should be three branches of the surface current crossing the northern Adriatic from the eastern to the western side; the northernmost one near the closed northern boundary of the Adriatic (along the line Venice-Trieste) is also of the interest to this work. During summer, both AIM and NASM show [*Zavatarelli and Pinardi*, 2003, Figure 15] that in the surface layer there is an outflow from the gulf to the rest of the northern Adriatic and an anticyclonic circulation in the inner part of the gulf. The difference between the results of the two models lies in the extent of anticyclonic circulation; while in the AIM this occupies the whole gulf, it is smaller, less intense and confined to the innermost coastline of the Gulf of Trieste in the NASM. The circulation in both cases turns the surface water mass from inside the gulf toward the northern Italian coastline at the gulf's entrance, where a narrow coastal belt (less than 5 km offshore) of enhanced outflow of a fresher water starts. This is the beginning of a coastline current, the northernmost branch of the E-W circulation of the northern Adriatic.

[5] During September the NASM shows a current field similar to the summer one, with the enhanced Istrian coastal countercurrent (ICCC) flowing southward along the Istrian peninsula. This was detected experimentally by computation of dynamic heights and current meter observations [*Supić and Vilibić*, 2006]. During September, NASM and AIM resulted in a surface circulation similar to that in the summer – an anticyclonic circulation inside the gulf (more enhanced and extending over the gulf in AIM) and a coastal outflow concentrated along the northern coastline outside

[1]Marine Biology Station, National Institute of Biology, Piran, Slovenia.

0148-0227/09/2008JC004904$09.00

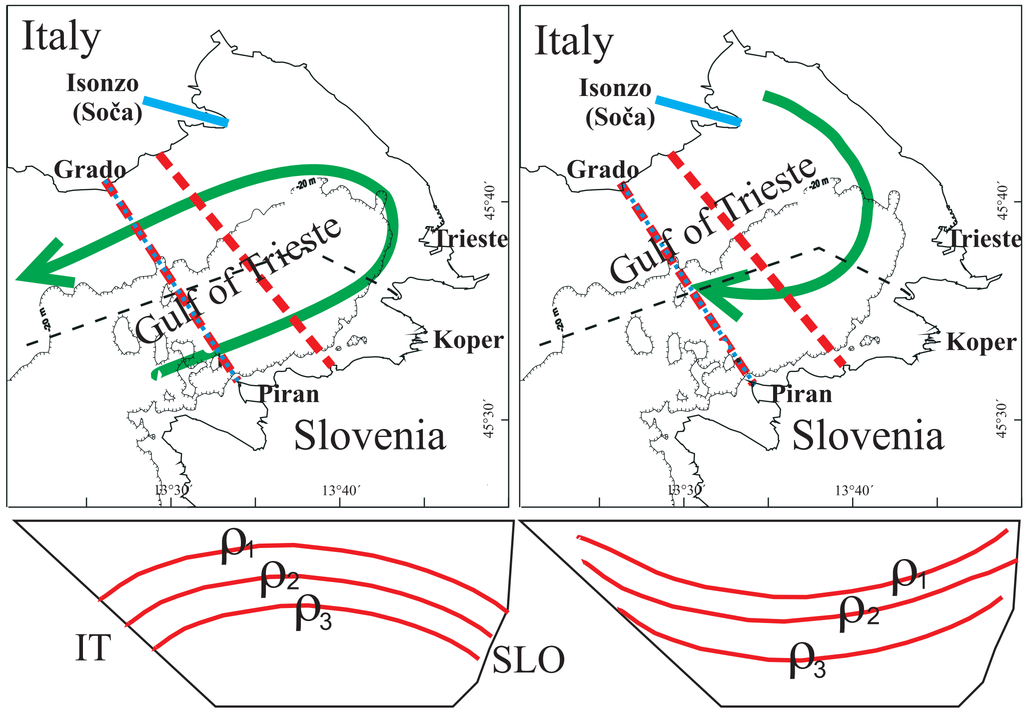

Figure 1. Sketch of possible circulation patterns during the stratified period in the Gulf of Trieste, the northernmost part of the Adriatic and Mediterranean Sea. (left) The cyclonic circulation with the "dome"-like (bottom) cross-section profile of density across the gulf's axis. (right) The anticyclonic circulation with the "bowl"-like cross section of the density. (top) The cross sections, along which the numerical model results are presented, are indicated by two dashed lines.

the gulf. NASM demonstrates only a weak link of the outflow to the ICCC near the southern coastline of the gulf. In September the ICCC is much stronger than during the summer period.

[6] The winter and spring circulation of the northern and central Adriatic Sea was also numerically simulated in a diagnostic mode with the Coupled Ocean/Atmosphere Mesoscale Prediction System [*Pullen et al.*, 2003], or COAMPS, where a 2-km resolution ocean model was forced by the inner and outer nests of the atmospheric model of coarser resolution. The period of simulations captured mainly the situations with the bora wind forcing in the winter-spring 2001 period, and the simulation with the forcing of higher resolution clearly reproduced the forced double-gyre (dipolar) circulation in the northern Adriatic, which is a consequence of the torque of the bora wind over the area and has already been detected by other authors [*Kuzmić*, 1991; *Kuzmić et al.*, 1985; *Orlić et al.*, 1986; *Paklar et al.*, 2001]. The variability of heat and momentum fluxes during bora episodes was presented with the COAMPS model [*Pullen et al.*, 2007]. However, a recent numerical study of the dynamics of the northern Adriatic, during and after the strong bora event, [*Cushman-Roisin and Korotenko*, 2007] revealed also some mechanisms of the circulation, among which the ICCC is a consequence of the baroclinic adjustment of the Istrian coastal waters following the bora wind impulse. It was also demonstrated that the bora, despite its strength (during winter), does not establish a wind-driven circulation that would be independent of the previous state, and that the circulation should be regarded as relaxations to sequential bora events.

[7] A comparison of the model results of circulation of the gulf during the winter period with bora with current meter measurements [*Malačič and Petelin*, 2006] demonstrated that heat fluxes at the surface have to be taken into account when space-time density variations are forecasted. That study, however, did not complete the circulation during winter and the spin-up period of a few years was not considered. The mechanisms of the direction of the surface outflow during winter will be thoroughly analyzed in this paper. Several details of the structure of the circulation inside the gulf and its exchange of the water mass with the rest of the Adriatic are still unknown because of two reasons. First, most of the circulation studies of the (northern) Adriatic with numerical modeling were not focused on the Gulf of Trieste. Second, the resolution of their numerical grid was too low, since the internal baroclinic Rossby radius can be as low as 2–3 km, as will be considered in section 5.

[8] Previous models also do not (and some of them could not) resolve the major dilemma about the circulation in the gulf during the stratified period (Figure 1), i.e., whether the circulation is cyclonic, with the typical "dome"-like profile of the density across the gulf's axis, or whether it is anticyclonic, with the "bowl"-like profile. The paper will show that the dilemma may be a false one and that the circulation is more complicated. The numerical concept with boundary conditions and the method of analysis of surface circulation during winter are described in section 2, which is followed by a description of results, the climatic circulation, in section 3. These are followed by comparison

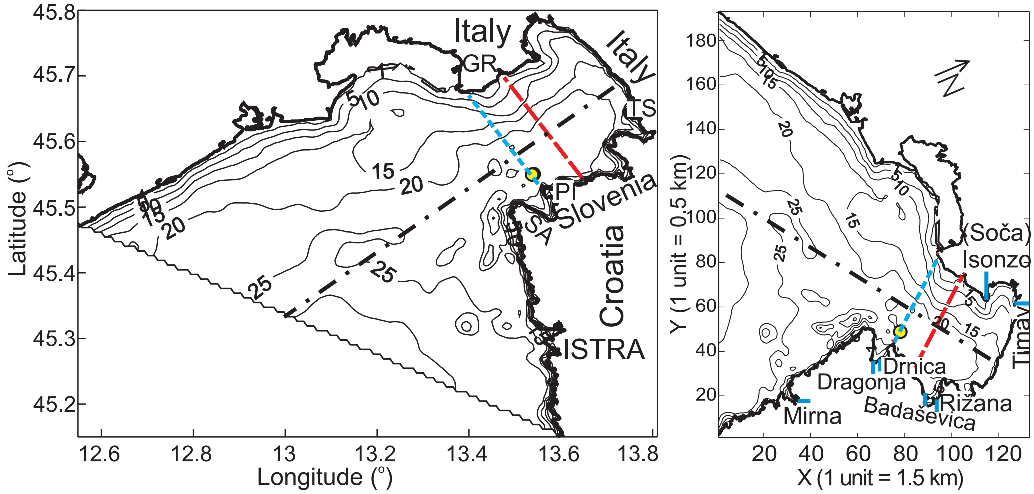

Figure 2. Map of the model domain of the Gulf of Trieste with its surroundings. (left) Geographic location; the towns Grado (GR) and Trieste (TS) (Italy), Piran (PI) (Slovenia), and cape Savudrija (SA) (Croatia) are shown. The latter lies at the northwesternmost edge of the Istrian peninsula. The yellow circle represents the position of a coastal buoy. The zigged line represents the open boundary line. (right) Model domain in model coordinates transformed in distances. Artificial river estuaries (blue lines), where river Soča (Slovenian) is also named Isonzo (Italian). The open boundary line is at the left edge of the domain. The dashed-dotted line represents the gulf's axis and the line of the vertical plane (profile) along the axis, while the blue and red dashed lines represent the location of vertical planes across the gulf's axis.

with other model results and measurements in section 4. The discussion and conclusions are listed in section 5.

2. Methods

2.1. Model Set Up

[9] The numerical model for the Gulf of Trieste (see Figure 2 for the model domain) is the Princeton Ocean Model [*Mellor*, 2003], applied in the models AIM and NASM for the whole Adriatic and the northern Adriatic, respectively [*Zavatarelli and Pinardi*, 2003]. The model calculates the vertical coefficients of momentum, heat and salinity from the second-order closure scheme of turbulence [*Mellor and Yamada*, 1982] and uses a sigma coordinate system. In a model for the gulf, 11 sigma layers (0, −0.06, −0.15, −0.26, −0.37, −0.48, −0.59, −0.70, −0.81, −0.91, −1.0) were applied, which are more densely packed near the surface, while the horizontal resolution of the model is 0.5 km. The model is one way nested in the NASM of the northern Adriatic Sea. The components of the wind stress [*Hellerman and Rosenstein*, 1983] were multiplied by a factor of 2.25 [*Zavatarelli et al.*, 2002], following suggestions of a previous study [*Cavaleri and Bertotti*, 1997] on the match of calculated stress from meteorological analysis and measured waves and currents (they increased the wind speeds of ECMWF for a factor 1.5, from which a factor $2.25 = 1.5^2$ yields). The model of the gulf is initialized with the interpolation on a model grid of initial state of the sea temperature and salinity, which are taken from the model results of a coarser NASM model of the northern Adriatic.

[10] At the sea surface the boundary condition for the vertical heat flux is

$$K_H(\partial T/\partial z)_\eta = [(1 - T_r)Q_S + Q_B + Q_H + Q_E]/(\rho_0 c_p), \quad (1)$$

where K_H is the vertical eddy coefficient of heat near the surface (Mellor-Yamada second-order closure scheme), $\eta(x, y, t)$ is the surface elevation, T_r is the transmission coefficient [*Jerlov*, 1976], Q_S the incoming solar (short-wave) radiation [*Reed*, 1977], Q_B the long-wave radiation [*Bignami et al.*, 1995], Q_H the sensible heat flux and the Q_E the latent flux, both being functions of the monthly mean temperature at the sea surface. They are computed by classical bulk formulae [*Kondo*, 1975]. ρ_0 is the density and c_p the heat capacity of the seawater.

[11] The vertical heat flux at the surface calculated by (1) usually gives model temperatures and salinities that deviate from objective analysis of the seasonal data. Therefore, in climatic models of circulation, the correction term $(\partial Q/\partial T)(T_\eta - T^*)$ is applied, where T_η is the surface temperature obtained by the model and T^* is the seasonal surface temperature (is T_{clim} in the code). This term was added in the brackets of the right hand side of (1). For the AIM model, $\partial Q/\partial T = 40$ W/(m^{2}K), which gives, for the annual heat budget of the Adriatic, a value of −11 W/m^2.

[12] The model of this paper was driven only from heat fluxes taken from the NASM model interpolated to a grid of 0.5 km for heat fluxes. In NASM a correction, $\partial Q/\partial T = 20$ W/(m^{2}K), was applied, giving a value close to zero for the annual heat flux over the northern Adriatic model, close to some other experimental findings [*Supić and Vilibić*, 2006], which show a net annual heat loss over the northern Adriatic of only −2.7 W/m^2 during the period 1966–2000. It was also pointed out [*Supić and Vilibić*, 2006] that the difference in surface heat fluxes in an east-west direction along the line Po river mouth (Italy)-Rovinj (Croatia) [*Artegiani et al.*, 1997] is between almost 10 W/m^2 during winter and 50 W/m^2 in autumn. An extensive study by *Supić and Orlić* [1999] led to values of annual heat loss along the eastern coastline that range (their Table 8) from

-4 W/m^2 (Rovinj) to -3 W/m^2 (Trieste) with an error 4–7 W/m^2 (their Table 7) for the period 1966–1992. In the model of the northern Adriatic [*Zavatarelli and Pinardi*, 2003], constant seasonal values of T^* and S^* were kept at the surface within the season in the equations for temperature and salinity. However, when consecutive images of currents and temperature fields were replayed, discontinuities in currents, temperature and salinity at appointed times between seasons were strong, sometimes with sudden removal of some gyres and the creation of others.

[13] Several model runs have been performed, with different values of the correction term $\partial Q/\partial T$ for the heat flux at the sea surface. No significant improvements in the circulation patterns were observed and we therefore ended the set of simulations by applying the heat fluxes at the sea surface (Q_S, Q_B, Q_H, and Q_E) provided by the NASM model, without correction term. This resulted in a net annual heat flux $Q = -1.6$ W/m^2, which is close enough to the value of -2.7 W/m^2 [*Supić and Vilibić*, 2006] where data spanned the period 1967–2000 (computed from their Table 1).

[14] In the model, all forcing fields at the surface (heat flux, precipitation-evaporation, and wind stress) varied linearly with time between monthly averages. Since linear variations between monthly values do not conserve the time integral of quantities, a correction procedure was applied on monthly averages [*Killworth*, 1996], and monthly pseudo values were utilized instead.

[15] In Figure 3, monthly mean values of heat fluxes were averaged over the model domain of the northern Adriatic as a result of the NASM model, and over the Gulf of Trieste, which resulted from the model of the gulf. Note that from January to May the upward heat flux at the surface (positive downward) without solar radiation is more negative for the northern Adriatic model than that for the gulf and is less negative between June and October. In Table 1 the monthly means of annual surface heat flux is listed, together with its standard deviations over the model domain; the latter have not been inserted in Figure 3 for clarity.

Table 1. Monthly Mean Solar Radiation Q_s, Net Annual Surface Heat Flux Q, and Evaporation Minus Precipitation ($E - P$), Averaged Over the Model Domain of the Gulf of Trieste[a]

		Q (W/m^2)		
Month	Q_S (W/m^2)	Gulf of Trieste	Northern Adriatic	$E - P$ (mm/month)
1	48 ± 3	−94 ± 91	−152 ± 89	54 ± 2
2	85 ± 5	15 ± 45	−18 ± 59	53 ± 1
3	140 ± 8	65 ± 26	44 ± 41	52 ± 1
4	208 ± 13	65 ± 24	49 ± 35	6 ± 4
5	255 ± 15	183 ± 35	197 ± 32	2 ± 3
6	303 ± 18	102 ± 28	112 ± 30	−40 ± 4
7	320 ± 19	116 ± 32	140 ± 31	−23 ± 4
8	264 ± 16	38 ± 34	65 ± 36	−7 ± 4
9	187 ± 11	−11 ± 31	25 ± 33	−2 ± 4
10	111 ± 7	−49 ± 23	−11 ± 31	−11 ± 6
11	58 ± 4	−337 ± 62	−340 ± 93	7 ± 5
12	41 ± 2	−112 ± 65	−109 ± 96	14 ± 5
⟨⟩±SD	168 ± 102	−2 ± 136	0 ± 145	9 ± 30

[a]For comparison the total heat flux over the domain of northern Adriatic is added. Standard deviations (SD) indicate space variations over the model domain. The last row contains the annual means and standard deviations of monthly means.

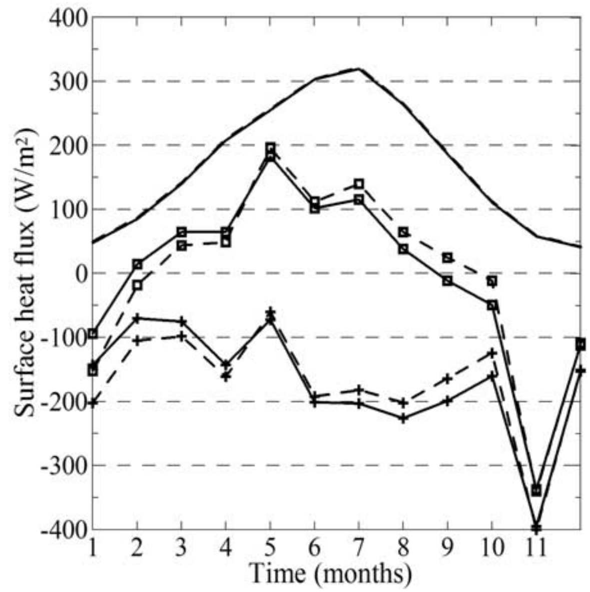

Figure 3. Evolution of monthly mean values of surface heat fluxes for the model of the Gulf of Trieste (solid lines) and for the model of the northern Adriatic (dashed lines). Solar input heat flux Q_S for the model of the gulf is represented by the solid line without symbols, while the dashed line without symbols, which represents Q_s over the northern Adriatic, is covered by the full line. The upward heat flux $-(Q_B + Q_H + Q_E)$ is composed of the long-wave radiation Q_B, the sensible heat flux Q_H, and the latent heat flux Q_E and is represented by the lines with crosses. The net annual surface heat flux $Q = Q_s - (Q_B + Q_H + Q_E)$ is represented by the lines with rectangles. Monthly mean values are averaged over the wet cells of the model domains. The annual average value for the total heat flux over the model of the northern Adriatic is close to zero, while the value for the model of the gulf is slightly negative, -1.6 W/m^2.

[16] The surface salinity flux is written as

$$K_H(\partial S/\partial z)_\eta = [E - P - R]S_\eta, \quad (2)$$

where S_η is the model predicted surface salinity, E is the evaporation, P the precipitation [*Legates and Wilmott*, 1990], and R the river input [*Raicich*, 1996]. In the models AIM and NASM of the Adriatic, $R \neq 0$ at points around the estuaries. Details about these surface fluxes can be found elsewhere [*Chiggiato et al.*, 2005; *Zavatarelli and Pinardi*, 2003]. It should be mentioned here that, in the model of the gulf, $R = 0$ in all model cells, as will be described below. The surface salinity flux (2) was corrected similarly to the heat flux, with an additional term proportional to ($S_\eta - S^*$), with a coefficient ($\Delta\sigma\ H\gamma$), where $\Delta\sigma H$ is the thickness of the surface layer, and γ = 1/day is the relaxation time, as in the model for the northern Adriatic [*Zavatarelli and Pinardi*, 2003].

[17] A word about the parameterization of river fluxes is appropriate. In the NASM model of the northern Adriatic the river fluxes were line distributed along the peninsula of Istria and along the northern (Italian) coastline of the gulf, mostly due to the poorly known river fluxes, to which the

Table 2. Monthly River Fluxes and Basic Geometry of River Estuaries Inserted in the Model[a]

Month	Mirna (m^3/s)	Dragonja (m^3/s)	Drnica (m^3/s)	Badaševica (m^3/s)	Rižana (m^3/s)	Timav (m^3/s)	Soča + Vipava (m^3/s)
1	10.6 ± 7.9	1.5 ± 1.7	0.5 ± 0.7	0.4 ± 0.3	5.2 ± 3.7	11.0 ± 6.7	101 ± 48
2	9.7 ± 7.2	1.5 ± 1.4	0.1 ± 0.1	0.2 ± 0.15	5.3 ± 4.3	10.7 ± 7.9	92 ± 50
3	8.7 ± 6.4	1.4 ± 1.1	0.1 ± 0.1	0.2 ± 0.1	5.2 ± 3.3	9.7 ± 6.6	105 ± 42
4	9.4 ± 5.5	1.5 ± 0.9	0.5 ± 0.4	0.4 ± 0.3	5.4 ± 2.6	10.2 ± 5.9	137 ± 42
5	6.1 ± 4.5	1.3 ± 1.7	0.2 ± 0.2	0.3 ± 0.2	3.5 ± 2.3	6.7 ± 5.2	129 ± 36
6	4.9 ± 4.4	0.5 ± ±0.7	0.06 ± 0.05	0.2 ± 0.2	2.9 ± 2.5	4.8 ± 3.5	118 ± 42
7	1.9 ± 1.5	0.2 ± 0.2	0.04 ± 0.03	0.09 ± 0.08	1.2 ± 1.0	2.2 ± 1.3	80 ± 31
8	2.1 ± 2.0	0.07 ± 0.08	0.01 ± 0.005	0.03 ± 0.02	1.2 ± 1.4	2.0 ± 1.9	63 ± 30
9	4.2 ± 4.4	0.2 ± 0.3	0.02 ± 0.02	0.16 ± 0.19	2.5 ± 3.3	4.1 ± 5.7	91 ± 56
10	7.7 ± 8.9	1.5 ± 2.3	0.2 ± 0.3	0.3 ± 0.3	4.3 ± 4.6	10.1 ± 10.7	127 ± 79
11	11.4 ± 7.7	1.8 ± 1.9	0.5 ± 0.6	0.5 ± 0.3	6.6 ± 4.0	14.7 ± 10.2	160 ± 80
12	10.4 ± 6.6	1.6 ± 1.6	0.5 ± 0.4	0.6 ± 0.4	6.4 ± 4.1	13.4 ± 9.0	121 ± 49
$\langle\rangle$±SD	7.3 ± 3.3	1.1 ± 0.6	0.2 ± 0.2	0.3 ± 0.2	4.1 ± 1.8	8.3 ± 4.2	110 ± 27
	Mirna (m^3/s)	Dragonja (m^3/s)	Drnica (m^3/s)	Badaševica (m^3/s)	Rižana (m^3/s)	Timav (m^3/s)	Soča + Vipava (m^3/s)
Period	1964–2003	1979–2000	1997–2000	1994–2000	1955–2000	1952–2000	1945–2000
Estuary length (m)	2500	2500	2500	2500	2500	3000	6000
Head depth (m)	2.0	2.0	2.0	2.0	2.0	2.0	4.0
Mouth depth (m)	3.0	5.0	5.0	3.0	11.0	4.0	7.5
Inclination (%)	0.04	0.12	0.12	0.04	0.36	0.07	0.06

[a]Average values of fluxes with standard deviations are in m^3/s suitably rounded. The river geometry is simplified to a rectilinear one with horizontal resolution of around 500 m, adapted to the model grid. River Mirna enters the northern Adriatic in Croatia, the Soča + Vipava (Isonzo + Vipacco) enters the Gulf of Trieste in Italy, while all other rivers enter the gulf in Slovenia. Monthly flows are given as monthly means (applied in the model) with standard deviations. The annual mean value of monthly flow rates with its standard deviation is denoted with $\langle\rangle$ ±SD. The data of artificial geometries of river estuaries applied in numerical model are also given. Data were provided by the Environmental Agency of the Republic of Slovenia, and the Meteorological and Hydrological Service of Croatia, Hydrology Division (river Mirna).

authors referred, in the previous study along the peninsula of Istria [*Raicich*, 1994]. However, by using these river data, initial simulations with the nested model of the gulf clearly showed a false narrow band of water mass with low salinity along its southern coastline and a better simulation of river fluxes became a necessity for a proper climatic study of the circulation. Therefore, a new table of monthly river fluxes was assembled (Table 2) for rivers that discharge in the Gulf of Trieste (east of the line Piran-Grado, see Figures 1 and 2 (right)). The annual average of monthly flow rates of the Soča + Vipava rivers (in Slovenian, Vipava discharges into the Soča), or the Isonzo + Vipacco rivers (in Italian), is around 110 ± 27 m^3/s, while the Isonzo outflow was estimated previously as 204 m^3/s [*Raicich*, 1994, 1996; *Zavatarelli and Pinardi*, 2003]. The diffused line source of freshwater along the peninsula of Istria is taken in their work as 187 m^3/s, while this study shows that it can barely be over 13 m^3/s. Since there is poor river outflow along the eastern Istrian coastline (not shown), almost all rivers along the Istria peninsula discharge either into the northern Adriatic or directly into the Gulf of Trieste, in the model domain. Data sources in this study are reliable as far as the peninsula of Istria is concerned. This difference of an order of magnitude in fluxes has consequences for the circulation pattern along the Istrian peninsula. In the model, the monthly mean values of river flows listed in Table 2 have been applied. However, the model domain covers a much larger area than the gulf, and river inflows from all sources along the northern Italian coastline between the Soča (Isonzo) River mouth and the end of the coastline in the model domain (the upper left corner of Figure 2 (right)) have been considered as described in the NASM.

[18] Rivers in the model of the gulf were considered in a manner that is different from that in AIM and NASM, where lower values of salinity were imposed on the surface cells around the river mouths, which were treated as regions with a higher precipitation rate. In this work the model topography was adapted to mimic the river estuary along the model grid line inside the land domain, where the width of estuaries equals the horizontal dimension of the grid cells (0.5 km). The geometrical characteristics of artificial river estuaries are presented in the bottom part of Table 2, while their locations are sketched on Figure 2 (right). We found, by numerical experiments, that it is sufficient to impose about ten model cells "upstream" from the river mouth along the estuary, with a topography that follows the topographical data where these are available. Otherwise, it is assumed that the depths of estuaries decrease linearly from the depth at the mouth toward a depth of 2 m at the upstream end. In this work, monthly values of river flow rates were imposed on the upstream-most cells in all sigma layers through the depth-averaged velocities in the downstream direction. The upstream-most velocity equals the flux divided by the vertical cross-section area in the upstream-most part of the artificial estuary. This approach is similar to that established in the study of the Rhône River plume [*Marsaleix et al.*, 1998]. The salinity in most upstream cells is zero. The sea surface elevation was extrapolated from the elevation in cells that neighbor the river mouths. This holds also for temperature, since climatic monthly temperatures of rivers in estuaries were not known.

2.2. Diagnostics of the Winter Conditions

[19] We assume that during winter stratification is not important for dynamics. Since in climatic studies wind changes are slow, we can reasonably suppose that local acceleration can be neglected. We will also suppose that advection terms with space variations of the velocity field are much weaker than the Coriolis term (Rossby number $\ll 1$).

This also implies that the horizontal friction (F_x, F_y) (where $F_x = \partial\tau_{xx}/\partial x + \partial\tau_{xy}/\partial y$, in which $\tau_{xx} = 2K_{MH}\,\partial u/\partial x$ and $\tau_{xy} = K_{MH}\,(\partial u/\partial x + \partial v/\partial x)$, and where the corresponding equation holds for F_y) is much smaller than the friction related to the vertical shear of velocity, because in POM the horizontal eddy viscosity K_{MH} is also dependent on horizontal velocity gradients according to Smagorinsky [*Mellor*, 2003; *Smagorinsky*, 1993]. The remaining terms of the Coriolis force, the pressure gradient force due to gradient in elevation and the friction due to vertical shear, can be expressed in terms of approximate velocity (u_0, v_0), where

$$\begin{aligned} v_0 &= (1/f)[g(\partial\eta/\partial x) - (\partial\tau_{xz}/\partial z)] \\ u_0 &= -(1/f)\left[g(\partial\eta/\partial y) - \left(\partial\tau_{yz}/\partial z\right)\right]. \end{aligned} \tag{3}$$

This velocity differs from the horizontal velocity (u, v), which is the solution of all terms in the equation of motion in particular because baroclinic effects have been neglected. The frictional stress (τ_{xz}, τ_{yz}) = $-(\langle u'w'\rangle, \langle v'w'\rangle) = K_{MV}\,(\partial u/\partial z, \partial v/\partial z)$, is a function of the model velocity (u, v), and not of (u_0, v_0). For the stress the coefficient of vertical eddy viscosity K_{MV} is calculated from the Mellor-Yamada parameterization scheme [*Mellor*, 2003]. However, K_{MV} cannot be calculated for levels that are closer to the sea surface than two σ levels. The elevation $\eta(x, y)$ also results from the model solution of the equation of motion with all relevant terms. This also means that the "true" velocity can be expressed as

$$\begin{aligned} v &= v_0 + (1/f)[(du/dt) - F_x] \\ u &= u_0 - (1/f)\left[(dv/dt) - F_y\right]. \end{aligned} \tag{4}$$

In this way the importance of the terms in brackets, e.g., the local acceleration, advection and horizontal friction, becomes clear. When stratification makes a significant contribution, terms of the baroclinic pressure gradient force

$$g/\rho_0(\partial/\partial x, \partial/\partial y)\left(\int_z^\eta \rho' dz\right)$$

also enter in brackets at the right-hand side of (4), in which $\rho'(x, y, z, t)$ is the density anomaly ($\rho = \rho_0 + \rho'$). Let us denote $-(v_0/u_0) = \tan\alpha_0$, where the ratio v_0/u_0 is obtained from (3). All terms on the right hand side of (3) are extracted from the model for the time centered on 20 January of perpetual year (winter situation). We will devote attention to the depth dependence of friction near the surface later; for now it is sufficient to point out that we are assuming (3) over the area of the surface boundary layer, away from side boundaries. If also $\tan\alpha = -(v/u)$, then both α_0 and α are functions of the horizontal positions (x, y). We look for the differences $\tan(\alpha - \alpha_0) = (\tan\alpha - \tan\alpha_0)/(1 + \tan\alpha\tan\alpha_0)$, applying (3) for α_0

$$\begin{aligned} &\tan(\alpha - \alpha_0) \\ &= -\frac{(v/u) + \left[(-g\partial\eta/\partial x + \partial\tau_{xz}/\partial z)/\left(-g\partial\eta/\partial y + \partial\tau_{yz}/\partial z\right)\right]}{1 - (v/u)\left[(-g\partial\eta/\partial x + \partial\tau_{xz}/\partial z)/\left(-g\partial\eta/\partial y + \partial\tau_{yz}/\partial z\right)\right]}, \end{aligned} \tag{5}$$

from which $\alpha - \alpha_0$ is calculated at each wet point (x_i, y_j), where $\eta(x_i, y_j)$ are calculated, while its horizontal gradients are calculated over the distance of two neighboring cells, $\partial\eta/\partial x \cong (\eta_{i+1,j} - \eta_{i-1,j})/(2\Delta x)$, and similarly for $\partial\eta/\partial y$. For points that neighbor the coastline, gradients are calculated only from two neighboring cells. Velocities (u, v) are calculated on the edges of cells around (x_i, y_j) and are therefore averaged on these points of η. The effect of omitted terms in (3) reflects also on the magnitude of velocity vectors, not just on their directions. For the measure of the relative deviation the following expression is accepted:

$$\delta_V = (|V| - |V_0|/|V_0|), \tag{6}$$

in which $|V| = (u^2 + v^2)^{1/2}$ is the magnitude of the resulting velocity at each (x_i, y_j), while the approximate speed $|V_0| = (u_0^2 + v_0^2)^{1/2}$.

[20] The final remark is related to the depth dependence of velocity and stress in (5) and (6). POM outputs turbulent viscosity K_{MV} two levels below the sea surface, which is extrapolated in the model to the first level and it outputs velocities at the intermediate sigma levels. When the uppermost stress is below the sea surface, the friction term is calculated in the following way:

$$\begin{aligned} (\partial\tau_{xz}/\partial z) &\simeq (\tau_{xz1} - \tau_{xz2}/z_{\tau1} - z_{\tau2}) \\ &= [K_{MV1}(u_1 - u_2/z_1 - z_2) - K_{MV2}(u_2 - u_3/z_2 - z_3)] \\ &\quad /(z_{\tau1} - z_{\tau2}), \end{aligned} \tag{7}$$

while, where the topmost stress is the boundary condition at the sea surface, $\boldsymbol{\tau}_1 = \boldsymbol{\tau}(0) = \boldsymbol{\tau}_s = 2.25\boldsymbol{\tau}_{wind}$ [*Cavaleri and Bertotti*, 1997]

$$(\partial\tau_{xz}/\partial z) \simeq [\tau_{sx} - K_{MV2}(u_2 - u_3/z_2 - z_3)]/(z_{\tau1} - z_{\tau2}) \tag{8}$$

and similarly for $\partial\tau_{yz}/\partial y$. Levels of stress ($z_{\tau i}$ for the ith level) that are equal to the levels of K_{MV} and of velocities (z_i) could be either sigma levels, or fixed. Four cases are analyzed in this respect. Velocities, however, are in intermediate levels between the levels of stress, unless the topmost stress is taken as given at the sea surface.

3. Results

[21] A review of the numerical results showed that it makes sense to group them in two sets of climatic seasons, the winter with autumn, which are weakly stratified seasons, and spring with summer, when the stratification is strong and plays a role over the whole domain, not just near the coastal front at the sea surface, as in winter. This pooling of results is also confirmed by the study on the penetration of heat [*Malačič*, 1991].

3.1. Weakly Stratified Seasons

[22] During winter the bora (burja) wind blows along the axis of the gulf and sweeps the surface water out from the gulf (Figure 4a (left), climatic mid-February; see also the black dashed-dotted line in Figure 2 for the definition of the axis). Because of the wind setup of the sea surface (higher

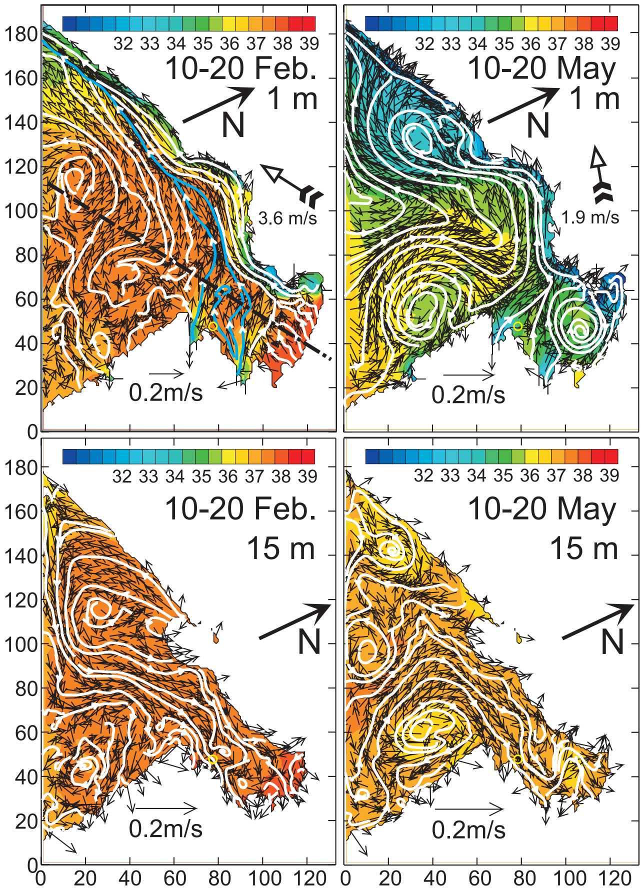

Figure 4a. Salinity and circulation of the Gulf of Trieste over the model domain, averaged over 10 day intervals during (left) winter (10–20 February) and (right) spring (10–20 May) of perpetual year at a depth of (top) 1 and (bottom) 15 m. Monthly mean climatic wind speed, averaged over the model domain, is represented by arrows with tails (Figure 4a (top)). Color bars of salinity are shown and the scale of currents is represented by an arrow in a blanked (land) area. White lines represent streamlines, blue lines mark the streamlines of the diagonal outflow at the surface during the winter period, and the black dashed-dotted line denotes the gulf's axis. The yellow circle represents the position of a coastal buoy.

near Venice, lower near Trieste), the pressure gradient force creates a return flow, the inflow near the seafloor (Figure 4a (bottom left)). However, at the surface this simplistic view during winter is complicated by the balance between the Coriolis force, the pressure gradient force and the friction. The fluid crosses the gulf diagonally (Figure 4a (top left), blue lines) from the southern (Slovenian) side toward the northern (Italian) side [*Malačič and Petelin*, 2006], where it joins the outflow of river freshwater. The latter is attached to the northern coastline and drives the water mass at the surface around the perimeter of the northern Adriatic toward Venice.

[23] The above qualitative assumption about the balance of forces is verified quantitatively. Figure 5 displays results for the deviation from the magnitude and direction of approximate velocity (u_0, v_0) for four different groups of levels for calculating the friction term near the sea surface. They are displayed in Table 3, together with summary statistics of results. In case 1, the depths of the first ($\sigma_2 = -0.06$) and second ($\sigma_3 = -0.15$) sigma layers below the sea surface are applied for the stress, while the intermediate depth between the two is the depth at which the velocity is defined. The distribution of approximate speeds in case 1 has a mean value (−11.9%) closest to zero, and is the narrowest with the smallest standard deviation (SD = 67.5%). Case 1 is the least asymmetric, although it is far from the normal distribution. It is also clear that cases 2 and 4 have sharp peaks of relative speed distribution close to the value −100%, which seems rather peculiar, since in case 2 the upper stress is taken at the sea surface, while in case 4 all levels are fixed (no sigma levels) and are below the sea surface. The distribution of directions of approximate velocities is also well centered in case 1 (the mean value of 9.0°), although in case 3 it is slightly better (7.2°), while the spread of directions around the mean value is best in case 1 (SD = 56.1°). There is also a pronounced bimodal distribution of approximate velocity directions in cases 2 and 4, with a larger peak around zero and a second around 100°, while in cases 1 and 3 the second peak around 150° is much smaller than the principal one.

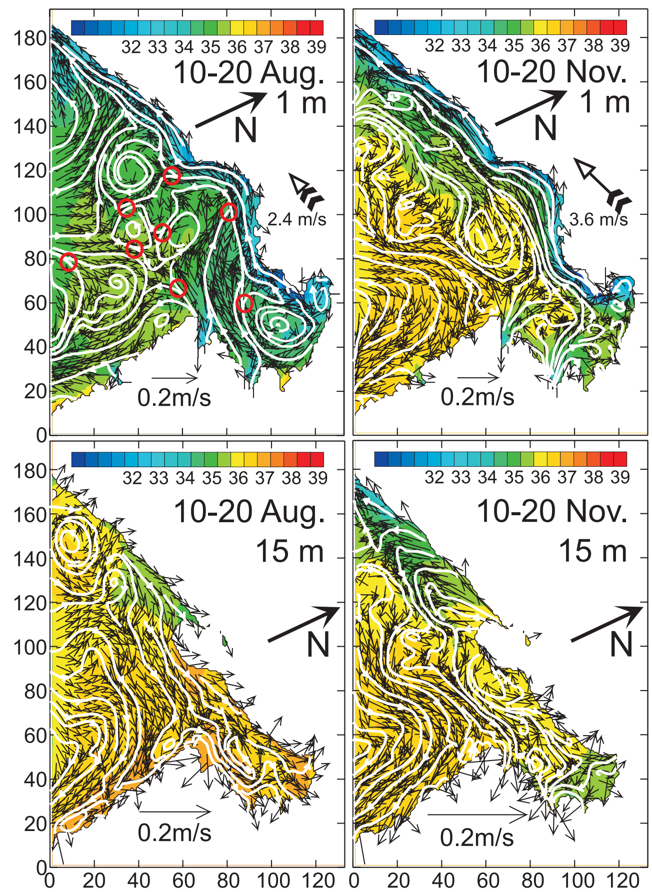

Figure 4b. As in Figure 4a, except for (left) summer (10-20 August) and (right) autumn (10-20 October) of perpetual year. Red circles in Figure 4b (topleft) mark the areas of bifurcations/amalgamations of jets/filaments between circulation gyres.

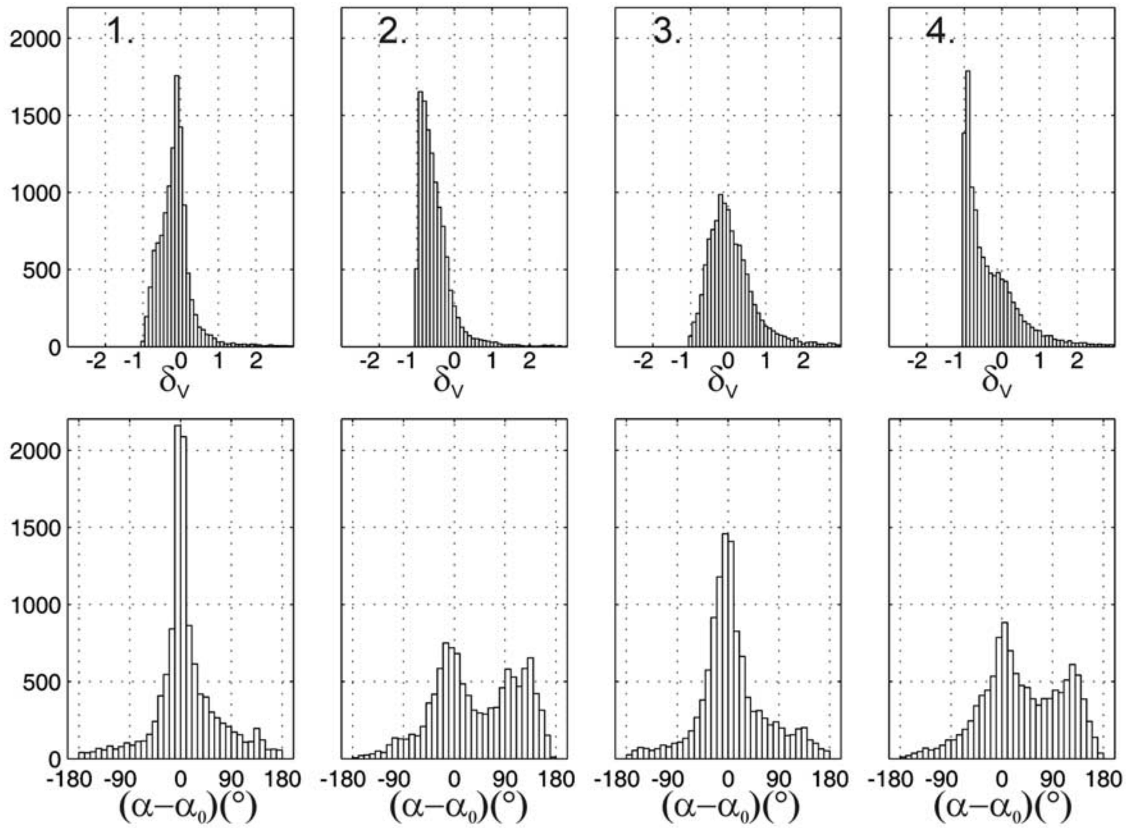

Figure 5. Statistical distribution of relative speed deviation δ_V (top) of the modeled velocity (u, v) from the speed $|V_0|$ of approximate velocity (u_0, v_0) and (bottom) of the deviation of direction ($\alpha - \alpha_0$). The velocity (u_0, v_0) results from (3). Four different types of calculation of vertical friction near the sea surface are listed in Table 3; plots in four columns correspond to four cases in Table 3. Calculations were performed over 12,160 model cells.

[24] During autumn (mid-November; Figure 4b (right)) the circulation is similar to that in winter. Again, there is a relatively narrow belt of surface freshwater. There are, however, also differences, like the noticeable surface jet-like outflows of fresh water that emerge from the small bays of Piran and Koper along the southern coastline. Model simulations without any river inputs (not presented here) showed that the diagonal crossing of the gulf from the southern coastline to the northern (Italian) coast in the N-W direction is still present during winter, but is absent during autumn, when the model shows the surface cyclonic circulation at the gulf's entrance, not the cyclonic gyre. However, at depth a small anticyclonic gyre 4–5 km in diameter in the southern (deeper) part inside the gulf is manifested (Figure 4b (bottom right)). During autumn there is also a southward flow along the peninsula of Istria (the ICCC), at the surface as well as in the depths (15 m), which was first noticed from density profiles [*Supić et al.*, 2000] and confirmed with the coarser model [*Zavatarelli and Pinardi*, 2003] over the area of the northern Adriatic. The model shows that this flow starts to develop already in (late) summer (mid-August; Figure 4b (left)). The vertical transects of density from the northern coastline to the southern one (Figure 6) show that in winter (Figure 6 (top)) in the bulk of the gulf, the freshwater stratification near the northern coastline is much more confined to surface layers and remains close to the coastline more than during autumn (Figure 6 (bottom)). In the latter season there is also a water mass of higher density near the sloped seafloor inside the gulf (Figure 6 (bottom right)), which is a consequence of the autumn cooling that is already completed during the climatic winter (Figure 6 (top right)), when the blob of denser water is

Table 3. Four Methods of Calculating Divergence of the Momentum Stress Near the Sea Surface[a]

	Case 1	Case 2	Case 3	Case 4
Level of $\boldsymbol{v}_1$	$(\sigma_1 + \sigma_2)/2$	–	–	−0.5 m
Level of $\boldsymbol{\tau}_1$	σ_2	σ_1	σ_1	−0.75 m
Level of K_{MV1}	σ_2	–	–	−0.75 m
Level of $\boldsymbol{v}_2$	$(\sigma_2 + \sigma_3)/2$	$Z = -1$ m	$(\sigma_1 + \sigma_2)/2$	−1 m
Level of $\boldsymbol{\tau}_2$	σ_3	$Z = -2$ m	σ_2	−1.25 m
Level of K_{MV2}	σ_3	$Z = -2$ m	σ_2	−1.25 m
Level of $\boldsymbol{v}_3$	$(\sigma_3 + \sigma_4)/2$	$Z = -3$ m	$(\sigma_2 + \sigma_3)/2$	−1.5 m
$\langle (v_1 - v_{10})/v_1 \rangle$ (%)	−11.9	−46.9	21.1	−15.2
SD$[(v_1 - v_{10})/v_1]$ (%)	67.5	82.3	159.3	256.4
$\langle \alpha - \alpha_0 \rangle$ (°)	9.0	39.2	7.2	36.6
SD$(\alpha - \alpha_0)$ (°)	56.1	74.4	60.2	71.9

[a]Cases 1 and 3 use the sigma levels, which are thicker in areas of larger depths; in case 4 the levels at fixed depth are considered. In cases 2 and 3 the surface stress is taken at the sea surface and given by $\boldsymbol{\tau}_1 = \boldsymbol{\tau}(0) = 2.25\boldsymbol{\tau}_{\rm wind}$, which is applied in the code as a boundary condition [*Zavatarelli and Pinardi*, 2003]. The three sigma levels which take part in calculations are $\sigma_1 = 0$ (sea surface), $\sigma_2 = -0.06$, $\sigma_3 = -0.15$, and $\sigma_4 = -0.26$. Calculations have been performed over 12,160 wet cells.

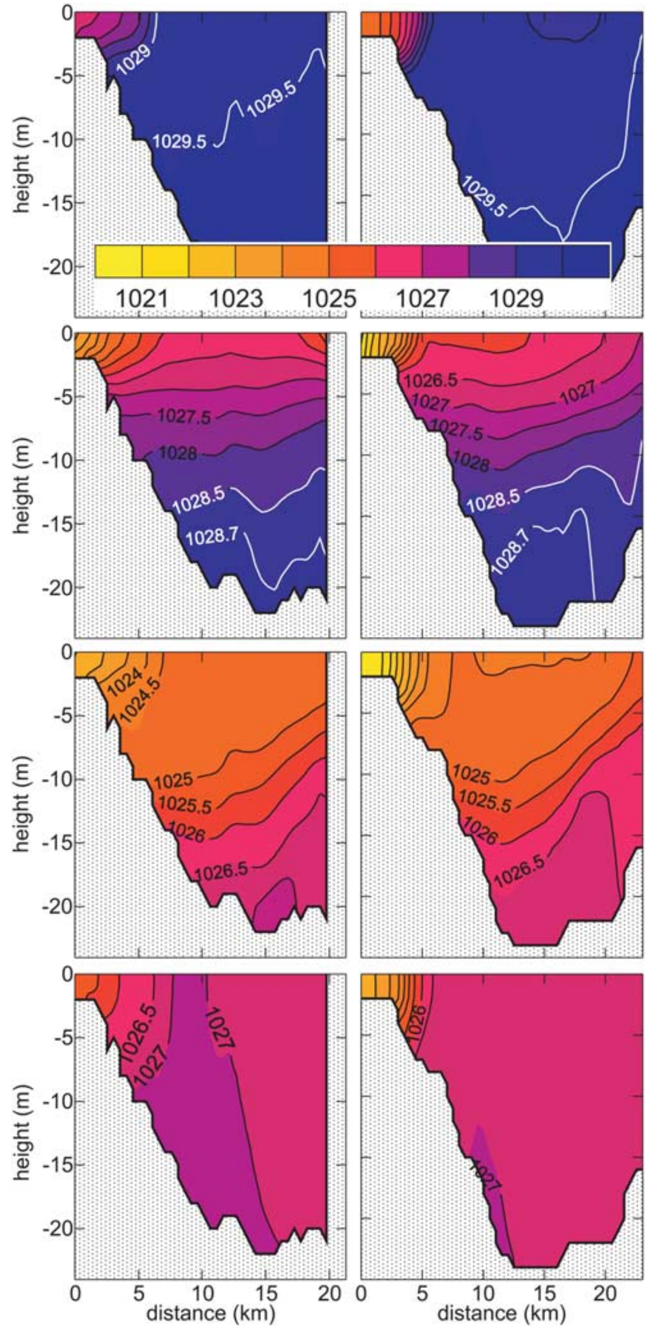

Figure 6. (left) Vertical cross sections of density from the northern (Italian) side at the gulf's entrance to the southern (Slovenian) coastline at the gulf's entrance (see Figure 2, dashed blue line) and (right) sections across the inner part of the gulf (see Figure 2, dashed red line). (top) Winter situation (climatic 10–20 February), (top middle) spring (10–20 May), (bottom middle) summer (10–20 August), and (bottom) autumn (10–20 November). The color scale of density is shown. The distance across the gulf is zero near the Italian side of the gulf.

no longer present in a much denser environment. The along-axis vertical profile of density (Figure 7) shows that during winter (Figure 7 (top)) the water inside the gulf is slightly lighter (see also Figure 6 (top right)) while during autumn (Figure 6 (bottom)) there is a column-like area of denser water, which is located outside the inner part of the gulf in front of the gulf' entrance (see the isobaths along the dashed-dotted line on Figure 2), broader near the seafloor and centered around the reef. There is one peculiar anticyclonic turn of current close to the seafloor during winter (Figure 4a), about 4 km from the coastal buoy in the offshore direction, which does not find its explanation in vertical profiles of density (Figure 6 and 7), and which seems to be topographically controlled.

[25] The vertical vorticity component ($\partial v/\partial x - \partial u/\partial y$) at 1 m depth (Figure 8) clearly demonstrates the freshwater belt along the northern coastline with negative vorticity (blue) during winter (Figure 8 (top left)) and autumn (Figure 8 (top right)), with its outer edge of positive vorticity (red color) due to horizontal shear. The negative horizontal divergence ($-\partial u/\partial x - \partial v/\partial y$) near the sea surface (Figure 8 (bottom left and bottom right)) is strongly positive in front of the Savudrija promontory (see Figure 2 for the location). There, $\partial w/\partial z > 0$; the vertical velocity increases with height near the sea surface, indicating a forced upwelling with bora wind. However, the hydrostatic POM did not clearly reproduce the upwelling in the innermost part of the gulf, where it is expected.

3.2. Strongly Stratified Seasons

[26] The circulation in spring (Figure 4a (right)), represented by climatic mid-May, looks similar to that in summer (mid-August, Figure 4b (left)). There is an anticyclonic circulation inside the Gulf of Trieste in the upper layer of the water column (Figure 4b (top)), which spreads down to 8 m below the sea surface. Two-dimensional streamlines show that the water in them is spinning clockwise toward the center, where the density is lowest. This center of the gyre with lowest density in the top part of the water column inside the gulf is slightly displaced from the gulf's center toward the northern coastline because of the Isonzo River outfall, which brings much more fresh water than the small rivers along the southern coastline (Table 2). During spring there are two anticyclonic vortices outside the gulf. The southern one near the coastline of the peninsula of Istria, which reaches depths of 15 m with the core of lowest density (salinity), vanishes during summer.

[27] At a depth of 15 m there is a marked inflow in the inner part of the gulf, with cyclonic departure in the gulf's interior and an anticyclonic one closer to the closed end of the gulf. In summer, there is an elongated cyclonic circulation at depth (15 m) in the central and southern parts of the gulf (Figure 4b (bottom left)). There is a cross flow near the surface at the gulf's entrance in spring and summer from the southern to the northern coastline, which was also seen during winter, although during spring it is more orthogonal to the gulf's axis. This cross flow is related to the anticyclonic gyre during warmer seasons and to the balance between Coriolis, wind stress and friction during winter.

[28] Vertical cross sections of density (Figure 6 (top middle and bottom middle)) show that during spring there is a dome-like density profile near the sea surface across the entrance to the gulf (Figure 6 (top middle left)), with lower densities near both coastlines. These profiles, however, are located at the western the edge of the anticyclonic gyre in the innermost (eastern) part of the gulf (Figure 4a (top right)), where the inflow-outflow in the surface layer is

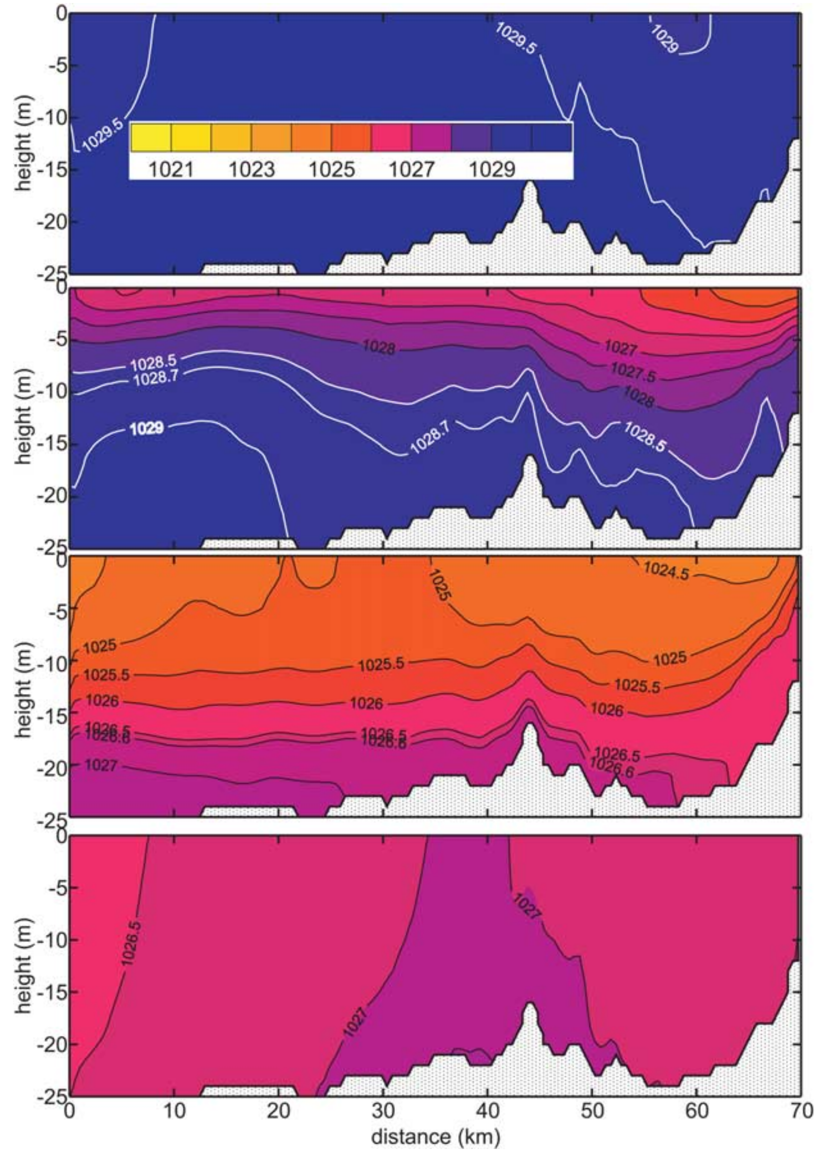

Figure 7. Vertical cross sections of density along the Gulf of Trieste (see Figure 2, dashed-dotted line). (top) Winter (climatic 10–20 February), (top middle) spring (10–20 May), (bottom middle) summer (10–20 August), and (bottom) autumn (10–20 November). The color scale of density is shown; the closed end of the gulf is on the right-hand side.

weak and the cross flow from the southern to the northern coastline dominates. During stratified seasons freshwater is practically absent from the southern (Slovenian) coastline, therefore the isolines of density are tilted upward toward the south, and they even break out at the surface (Figure 6 (top middle and bottom middle right), right side of x axis). A dome-like structure of density is then present at depths below 14 m (Figure 6 (top middle right) the density isoline of 1028.5 kg/m^3; and more pronounced in Figure 6 (bottom middle right) the density isoline of 1026.5 kg/m^3) with a maximum closer to the southern part of the gulf. This density distribution agrees with the cyclonic circulation at depth, with an inflow closer to the southern coastline (Figures 4a (bottom right) and 4b (bottom left)).

[29] The vertical cross section along the gulf's axis (Figure 7) shows that in spring (Figure 7 (top middle)), there is a bowl-like vertical profile of density in the upper part of the water column, which roughly agrees with the anticyclonic surface circulation, while at depths below 17 m, at a distance 50–60 km from the open boundary line (x axis) there is roughly a dome-like density profile inside the gulf, which agrees with the cyclonic turn (Figure 4a (bottom right) of currents at those depths. East of the dome structure is a bowl-like structure (Figure 7 (top middle), distance 55–65 km) at depth, near the closed eastern end of the gulf, which again agrees with the circulation (Figure 4 (bottom right)) that makes the anticyclonic turn at depths. The isoline of 1028.5 kg/m^3 (Figure 7 (top middle)) peaks sharply to a depth of 10 m at a distance of 67 km. We see that in summer (Figure 7 (bottom middle)), the bowl-like shape of isolines (1025 kg/m^3) of density in the surface part of the water column also extends outside the entrance of the gulf, almost 10 km westward from the position of the ridge

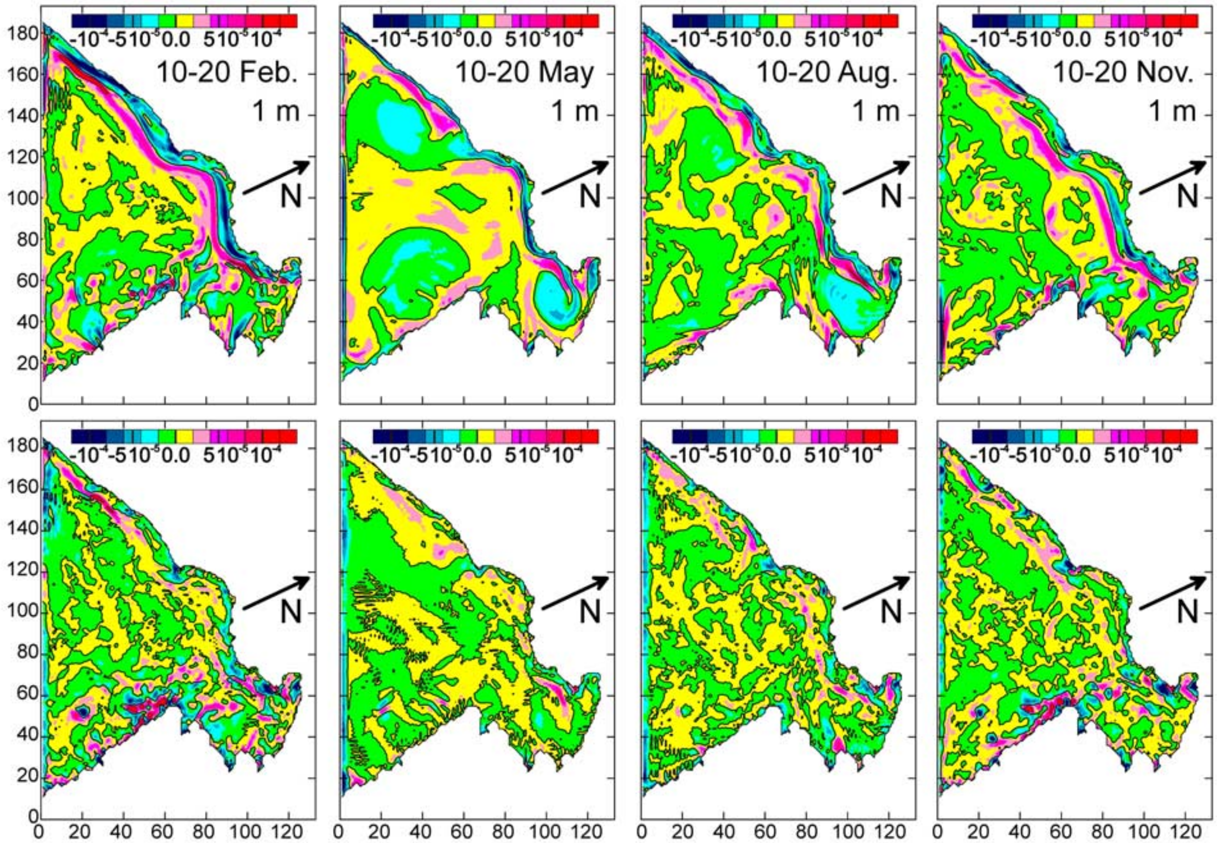

Figure 8. Vertical component (top) of vorticity $\partial v/\partial x - \partial u/\partial y$ and (bottom) of negative horizontal divergence $-\partial u/\partial x - \partial v/\partial y = \partial w/\partial z$ at 1 m depth for climatic (left) winter (10–20 February), (left middle) spring (10–20 May), (right middle) summer (10–20 August), and (right) autumn (10–20 November) for the climatic circulation in the Gulf of Trieste. Color bars are shown.

at the entrance. It is clear from Figure 7 that vertical profiles of density along the gulf's axis during warmer seasons is influenced by topography (by the ridge at 16 m depth at a distance of 43 km and by the closed side of the gulf at a distance of 70 km from the open boundary line), as well as by the outflow of the Isonzo River and seasonal warming. Since the circulation at depth is mostly directed along the gulf's axis, with weak components that cross the gulf, we cannot expect strong links between the density profiles along the gulf's axis and currents across the gulf's axis. The ridge at the gulf's entrance spikes the density isolines to shallower depths and separates the density structure at depths inside the gulf from that outside it. In autumn (Figure 7 (bottom)), when surface cooling starts the convective overturning, the density is quite homogeneous, apart from a broad cone-like structure of slightly larger density outside the gulf, centered at distance 38 km from the open boundary of the model, about 5 km westward of the ridge in front of the gulf's entrance.

[30] The coastal "red" belt of positive vorticity at the surface along the northern coastline during winter is interrupted in spring by two anticyclonic vortices (Figure 8 (top left middle)), and by just one in summer (Figure 8 (top right middle)). They stretch the negative vorticity (blue) in the interior of the model domain. The anticyclonic vortices in spring have the most homogeneous vorticity, the reason for which is as yet unknown. During summer, however, there are also vortices on a scale of a few km (the internal Rossby radius of deformation $R_0 \sim 2$ km, see Discussion), between which there are jets that exchange the water between them. It appears that the fluid particles in these jets follow the conservation of potential vorticity, which is evidenced by several amalgamations and bifurcations of their paths (Figure 4b, red circles). The Coriolis parameter (planetary vorticity) is constant over this small domain. Assuming, to a first approximation, that the density does not vary much horizontally (see Figure 7 for the location of the areas in which this approximation holds), the conservation of potential vorticity in the upper layer leads to the conservation of relative vorticity. The latter is composed of two contributing terms, the centrifugal term due to the curvature of the fluid particle's path, and the shear term. The balance between them results in jet meandering, separation of particles from it (bifurcation of jets) and seizure of other particles in them (amalgamation of trajectories) [*Cushman-Roisin*, 1994]. This very crude approximation certainly does not hold near the coastline. It does, however, give a first impression about the mechanisms causing complicated streamlines during summer. In Figure 8 (top right middle) the relative vorticity in places of meanders between gyres is mostly weak during summer, with absolute values below 10^{-5}/s (green and yellow colors). This does not mean that the shear inside

the meanders is weak, but that it is compensated by the turning of meanders in such a way that the relative vorticity is kept small.

4. Comparison With Other Model Results and Measurements

[31] Comparison of the climatic model with measurements is extremely hard, since a long period of measurement is required. However, the model results during winter, when a steady bora wind blows, have already been compared with measurements [*Malačič and Petelin*, 2006] and are not repeated here. There was a qualitative agreement of model results with measurements (outflow near the surface, inflow at depth). The same holds for the situation in spring. Along the southern part of the entrance to the gulf, there is an inflow at all depths except near the sea surface where the current is oriented toward the northern (Italian) coastline [*Malačič and Petelin*, 2001] (their Figure 8–6). Both characteristics of spring flow are reproduced with the present model (Figure 4a (right), currents around the yellow circle). Also observations of circulation in the Bay of St Georges [*Drinkwater*, 1994] are similar to the results presented in this work, when the wind is blowing in summer along the bay's axis from its head to its entrance.

[32] Very similar circulation at the surface during bora wind has also been reproduced numerically by another model [*Crise et al.*, 2006] having a completely different architecture (MIT general circulation model). That model was set up for the synoptic circulations, and its domain covers only the interior part of the gulf (the open boundary line is placed along a line connecting the cape of Piran with Grado). The model was initialized with different fields of temperature and salinity and with the application of boundary conditions that differ from the ones applied in this study. With that model the detaching of the surface current from the southern coastline, with its diagonal crossing of the gulf toward the northern coastline outside the gulf, was also reproduced for the bora wind event during winter. Moreover, simulations of synoptic circulation during bora in summer, with a strongly stratified water column [*Querin et al.*, 2007], also reproduced the rightward declination of surface current in the central part of the gulf, which resembles the diagonal cross flow.

[33] A set of numerical simulations, performed by another group [*Dorić*, 2008] with numerical models that are structured on completely different numerical schemes (Mike 3 and PCFLOW3D) also demonstrates a very similar deviation of the surface current to the right from the wind direction during the bora episode, compensated by an inflow at depths, which agrees with one of the first simulations of synoptic circulations of the gulf (R. Rajar, Three dimensional modelling of currents in the northern Adriatic Sea, paper presented at 23rd Congress, International Association for Hydraulic Research, Ottawa, 1989). All these different numerical simulations strongly support this deviation of the surface current, which should be verified experimentally.

[34] During spring the cyclonic circulation at depth (Figures 4), related to the dome-like density distribution (Figure 6 (top middle and bottom middle right)) has already been addressed [*Malačič and Petelin*, 2001, Figure 6–4 and 6–5], when hydrographic measurements were examined. A similar distribution of density as in Figure 6 (right) was obtained decades ago [*Mosetti*, 1967] for the August–September 1966 campaign, as well as during the Alpe-Adria campaign [*Celio et al.*, 1991]. In a more recent objective analysis of the decadal trends of temperature and salinity and their horizontal distribution in the gulf [*Malačič et al.*, 2006], where data covering only the last few decades (1991–2003) was used, the horizontal distribution of salinity at the surface [*Malačič et al.*, 2006, Figures 7–10] showed a wide (6–12 km offshore) belt of freshwater, caused by Isonzo discharge during summer, and especially, in autumn. In winter the freshwater belt is narrower (3–5 km), while in summer (and spring) the clear signal of the offshore extension of the bulge of Isonzo freshwater is missing. This sheds some doubt on the results of the numerical model for summer season. However, we have to remember that the source data in both studies cover very different periods, where the ATOS data (1911–1992) of temperature and salinity, to which the model is being "nudged", are more representative for the proper climatic state.

[35] The anticyclonic circulation at the surface during stratified seasons has not been confirmed experimentally so far, although there have been some hints in this direction [*Sanay and Valle-Levinson*, 2005; *Stravisi*, 1983; *Stravisi et al.*, 1981]. This circulation, however, also resembles the circulation in another gulf, which is partially filled with a plume of river freshwater [*Fujiwara et al.*, 1997]. The explanation given there also follows the conservation of potential vorticity, with the inclusion of entrainment of fluid from the layers at depth into the surface layer. At depths, however, the circulation looks similar to that found in this study during winter.

[36] In another numerical work [*Pullen et al.*, 2003] that covers the circulation of the northern Adriatic during winter and part of the summer period, the first mode of the empirical orthogonal function (EOF) of velocity [*Pullen et al.*, 2003, Figure 13] shows that, at a depth of 5 m, there is an inflow in the gulf along the northern coastline of the Istrian peninsula (southern coastline of the gulf), and an outflow along the northern coastline of the gulf. From the plot of the first EOF mode of currents for the depth of 25 m, one can deduce that there is an inflow in the gulf near the sea bottom, which is mostly at depths shallower than 25 m. These results are very similar to those presented in this work.

5. Discussion With Conclusions

[37] Although there have been a number of studies in the last few decades related to the wind driven circulation in shelf areas and large lakes [*Csanady*, 1982], novel findings about this circulation are still appearing from semianalytical [*Winant*, 2004] and numerical [*Sanay and Valle-Levinson*, 2005] studies. The latter study showed that, in a gulf of triangular or Gaussian cross section, there is an axially symmetric transverse circulation structure in the vertical cross-section plane. This was convergent toward the upwind flow in the central part of the gulf, while the downwind flow was present along the shoals, when no rotation of the Earth was included. When the rotation was included, they found that the gulf's dynamics depend on the ratio of its maximum

depth and the Ekman depth. If this ratio is close to or less than one, the circulation structure is similar to the nonrotating case, while for higher values the flow in a semi-enclosed basin of symmetric cross section becomes asymmetric: maximum downwind flow is located closer to the right hand side shoal, which resembles the circulation found in this study (Figure 4a (top left)). However, in that numerical study [*Sanay and Valle-Levinson*, 2005] the focus was on a cross-sectional structure of circulation in a semi-enclosed basin, and not on the rightward declination of surface current from the downwind direction.

[38] The Ekman depth $D_E = \pi(2K_{MV}/f)^{0.5}$ in the Gulf of Trieste can be estimated directly from the wind speed without K_{MV}, since $(\tau_{yz})_0 = (K_{MV}\ \partial v/\partial z)_0 \cong (\rho_a/\rho_w)C_D U_{10}^2$, in which we insert the component of the Ekman velocity $v = V_S \exp(\pi z/D_E) \cos(\pi/4 - \pi z/D_E)$, which yields $(V_S/U_{10}) = 2^{0.5}\pi(\rho_a/\rho_w)C_D U_{10}/(fD_E)$. The velocity magnitude can be related to the wind speed [*Csanady*, 1982] $V_S = kU_{10}$, where $k \cong 0.03$, meaning $D_E = 2^{0.5}\pi(\rho_a/\rho_w)C_D U_{10}/(fk) \cong 4.6\ U_{10}$, where $\rho_a/\rho_w = 1.25/1027$; $C_D = 2.6\ 10^{-3}$ and $f = 1.03\ 10^{-4}$/s. For $U_{10} = 3.6$ m/s (climatic wind during winter) $D_E \cong 16$ m and since the depth $H \cong 22$ m at the southern side of the gulf, where the deviation of the surface current to the right of the wind is noticed, $H/D_E \geq 1$ (also with other reasonable values of k and C_D), which agrees with the mentioned study [*Sanay and Valle-Levinson*, 2005].

[39] However, horizontal dimensions of structures simulated by the model can be estimated by the internal Rossby Radius of deformation R_0. Since we are interested in the interior part of the gulf, three points along the red and blue cross-section lines (Figure 2) have been chosen for the analysis of the vertical distribution of buoyancy frequency. Two points out of three are about 2 km away from the end points of each cross-section line, while the third point lies in the middle of each cross section. Vertical profiles of buoyancy frequency along these six points present sufficient statistics for the estimate of R_0 [*Kundu*, 1990], calculated numerically (J. Klinck, online material, 1999, available at http://woodshole.er.usgs.gov/operations/sea-mat/), where only the first (the largest) internal speed c_i was considered, from which the largest $R_0 = c_i/f$ follows. R_0 ranges between 0.56 and 2.68 km, or 1.59 ± 0.65 km as an average value with SD. During winter values are between 0.56 and 1.54 km (1.12 ± 0.36 km), while the largest are during spring, between 1.46 and 2.68 km (2.16±0.50 km), followed closely by values during summer with lower amounts of river freshwater. Resultant structures of vortices correspond to these values (Figures 4a, 4b, and 8). Values of R_0 indicate that the model's horizontal resolution of 0.5 km is at the edge of the lower limit of R_0 and that coarser models would certainly not be accurate enough to capture vortices of size R_0. The POM model may also perhaps mix the surface part of the water column too much, what artificially decreases R_0. This does not, however, affect general conclusions about the dimensions of vortices with respect to the dimensions of the Gulf of Trieste.

[40] What can we conclude from the analysis of surface circulation during climatic winter, where results for the approximate velocity in case 1 are similar to those in case 3 (sigma layers), and those in case 2 are qualitatively similar to those in case 4 (fixed depths). The steady state approximation of surface dynamics during the climatic winter, in which advection and horizontal friction are neglected, makes sense over the inner part of the modeled area away from boundaries. However, the major problem is how to calculate the vertical friction between neighboring layers. It is obvious that vertical gradients applied on sigma levels give better results than those applied on fixed depths for POM, and that it is better to use the (sigma) level below the sea surface for the uppermost stress. Nevertheless, the range of mean values of relative deviation of approximate speeds around the modeled ones in the four cases is from −47% to 21%, with the SD ranging from 68% to 256%. The mean deviation of directions varies between 7° and 39°, with SD between 56° and 74°. The approximate velocity (u_0, v_0) of the stationary circulation does not take into consideration any pressure gradient force due to variations in density. Moreover, near the northern (Italian) coastline there is a narrow belt of river freshwater (Figure 4a (top left)) which, with the baroclinic pressure gradient force, affects the dynamics and is not accounted for in (u_0, v_0). The statistics for the deviation of approximate velocity (u_0, v_0) from the modeled one (u, v) confirm that the dynamics of the upper layer during climatic winter may be considered, to a first approximation, to follow that of the steady surface boundary layer. The statistics, however, were conducted on all wet cells of the model (12160), also on those which border on the coastline, where the flow is directed along it.

[41] When the river freshwater inflows are enhanced, the gulf behaves like a ROFI (Regions of Freshwater Influence) domain [*Fujiwara et al.*, 1997]; and the northern half of the gulf is occupied by the inertial plume with anticyclonic circulation at the surface. The upward entrainment of the lower water mass at the base of the upper layer causes the horizontal divergence and an increase of the total surface outflow (not the freshwater outflow), which is much larger than the flux of the Isonzo (Soča) River. This necessitates a return inflow in the lower layer. In the case of the Gulf of Trieste the upward slope of the surface pycnocline from the northern to the southern coastline, the dome-like density distribution near the sea bottom and the coastline barrier at the eastern side relate to an estuarine-like circulation at the surface, with cyclonic circulation at depth.

[42] Another study found that in the Hudson Strait [*Ingram and Prinsenberg*, 1999] which connects Hudson Bay with the Atlantic ocean (Labrador Sea), there is also a cyclonic circulation system (there in late summer) with a dome-like density profile at depth and an upward tilt of isolines of density offshore the coastline filled with fresher water, similar to the here described situation during spring and summer in the gulf's interior. However, we also observed numerically that there is also a match of an anticyclonic turn at depth near the closed, eastern end of the gulf in spring and summer: a clear bowl-like profile between the mouth of the Isonzo River and the promontory south of Trieste is present below a depth of 7 m during spring and summer (not shown).

[43] A numerical study of river plumes [*Isobe*, 2005] with POM shows that the core of the inertial bulb in front of the Isonzo River mouth would be inertially unstable and that the ballooning of the inertial plume is limited by the rectifying (tidal) current. For this reason we intend to add the tidal dynamics into the climatic circulation of the Gulf

of Trieste in the near future, since it is expected that during the spring tide the offshore extent of the inertial plume would be less than during the neap tide. The bora wind stress acting along the gulf's axis limits the offshore spread of the inertial bulb of fresh water from the Isonzo, and some indications of this are visible from model results (Figures 4, winter and autumn situations, when bora blows). However, simulations with strong river outflow and strong bora wind have to be conducted.

[44] A recent numerical study [*Querin et al.*, 2007] shows that the Isonzo plume spreads radially offshore (spring 2004) after the peak outflow and after the decrease of the southern wind. The plume then occupies a large proportion of the inside part of the gulf. The circulation within the inertial plume is anticyclonic while, near the surface front at the plume's edge, there is a convergent flow with strong horizontal shear; the surface flow south of the front (outside the plume) is flowing northward to the front. However, this case cannot be considered to support the anticyclonic circulation pattern during summer, when the river flow is relatively weak.

[45] Findings of this study for circulation during winter have been shown to have some theoretical basis, and are also confirmed by other examples of studies and modeling. It was shown that the diagonal surface circulation from autumn to spring is generally influenced by the bora wind and the Coriolis and pressure gradient forces. This rightward declination of the wind-driven surface current from the downwind direction is the most prominent feature of the model, while at depths there is a compensating inflow current.

[46] In the depths, however, model analysis has shown that, in stratified seasons, the cyclonic turns and gyres are related to the dome-like density profile across the gulf in its interior, which is governed by temperature. At the surface, however, there is a dominant anticyclonic circulation with lower salinity related to the inertial bulge of fresher water, which mostly originates from the Isonzo (Soča) River.

[47] Contrary to the effect of the Isonzo River outflow at the northern coastline, the smaller river outflows which emerge from the heads of opened bays along the southern coastline exert a less important influence on surface circulation. Their freshwater spreads across the whole gulf to the northern side in a thin, narrow and buoyant, jet-like structure, which also appears to be present when their fluxes are not at their peak values. These features have not yet been observed and deserve further attention. Jets of freshwater that emerge from rivers along the southern (Slovenian) coastline during colder seasons are reflections of surface diagonal outflow circulation (as trails of a passive tracer) and do not significantly affect it.

[48] At depth the cyclonic turn of current during stratified seasons is followed by the anticyclonic turn of current near the closed end of the gulf. We observed numerically that even in such a small semienclosed gulf of dimensions 20 $\times$ 20 km and depths shallower than 24 m the ratio between the typical length of the gulf L = 20 km and R_0 is about 10, indicative enough for a conclusion that a small gulf may be loaded with vortices and that its circulation is far from being simple, especially during the stratified period, despite its smallness. The model reproduced the dome-like density structure associated with cyclonic turns and the bowl-like structure with anticyclonic turns. Since a cyclonic turn of inflow inside the gulf near the seafloor is also seen during winter, the topography may also contribute to the pathway of circulation. This is left for future studies.

[49] **Acknowledgments.** This research is part of a research program funded by the Ministry of Higher Education and Technology of Slovenia (contract P1-0237), the Italian Ministry for the Environment and Territory (the ADRICOSM project), the UNESCO-IOC (the ADRICOSM-EXT project), and the EU funded INTERREG IIIa IT-SLO project "ISMO". We are indebted for the river flux data to Igor Strojan from the Environmental Agency of the Republic of Slovenia and especially to Ksenija Cesarec from the Meteorological and Hydrological Service of Croatia, Hydrology Division.

References

Artegiani, A., D. Bregant, E. Paschini, N. Pinardi, F. Raicich, and A. Russo (1997), The Adriatic Sea general circulation. Part I: Air sea interactions and water mass structure, *J. Phys. Oceanogr.*, *27*, 1492–1514, doi:10.1175/1520-0485(1997)027<1492:TASGCP>2.0.CO;2.

Bignami, F., S. Marullo, R. Santoleri, and M. E. Schiano (1995), Longwave radiation budget in the Mediterranean Sea, *J. Geophys. Res.*, *100*, 2501–2514, doi:10.1029/94JC02496.

Cavaleri, L., and L. Bertotti (1997), In search of the correct wind and wave fields in a minor basin, *Mon. Weather Rev.*, *125*, 1964–1975, doi:10.1175/1520-0493(1997)125<1964:ISOTCW>2.0.CO;2.

Celio, M., J. Faganeli, S. Fonda-Umani, J. Forte, V. Malačič, R. Melis, and F. Sanzin (1991), Variation of hydrological parameters, nutrients, and particulate matter in the Gulf of Trieste (northern Adriatic) in the period March-July 1990, report, p. 12, Osserv. dell'Alto Adriatico, Trieste, Italy.

Chiggiato, J., M. Zavatarelli, S. Castellari, and M. Deserti (2005), Interannual variability of surface heat fluxes in the Adriatic Sea in the period 1998–2001 and comparison with observations, *Sci. Total Environ.*, *353*, 89–102, doi:10.1016/j.scitotenv.2005.09.031.

Crise, A., S. Querin, and V. Malačič (2006), A strong bora event in the Gulf of Trieste: A numerical study of wind driven circulation in stratified conditions with a pre-operational model, *Acta Adriat.*, *47*, 185–206.

Csanady, G. T. (1982), *Circulation in the Coastal Ocean*, 279 pp., D. Reidel, Dordrecht, Netherlands.

Cushman-Roisin, B. (1994), *Introduction to Geophysical Fluid Dynamics*, 320 pp., Prentice Hall, Englewood Cliffs, N. J.

Cushman-Roisin, B., and K. A. Korotenko (2007), Mesoscale-resolving simulations of summer and winter bora events in the Adriatic Sea, *J. Geophys. Res.*, *112*, C11S91, doi:10.1029/2006JC003516.

Dorić, E. (2008), A comparison of the MIKE 3 and PCFLOW3D models for hydrodynamic simulations in the Gulf of Trieste, B. Sc. thesis, Univ. of Ljubljana, Ljubljana, Slovenia.

Drinkwater, K. F. (1994), The response of an open stratified bay to wind forcing, *Atmos. Ocean*, *32*(4), 757–781.

Fujiwara, T., L. P. Sanford, K. Nakatsuji, and Y. Sugiyama (1997), Anticyclonic circulation driven by the estuarine circulation in a gulf type ROFI, *J. Mar. Syst.*, *12*, 83–99, doi:10.1016/S0924-7963(96)00090-5.

Hellerman, S., and M. Rosenstein (1983), Normal monthly wind stress over the world ocean with error estimates, *J. Phys. Oceanogr.*, *13*, 1093–1104, doi:10.1175/1520-0485(1983)013<1093:NMWSOT>2.0.CO;2.

Ingram, R. G., and S. Prinsenberg (1999), Coastal oceanography of Hudson Bay and surrounding eastern Canadian arctic waters, in *The Sea: The Global Coastal Ocean: Regional Studies and Synthesis*, edited by A. R. Robinson and K. H. Brink, pp. 835–861, John Wiley, New York.

Isobe, A. (2005), Ballooning of river-plume bulge and its stabilization by tidal currents, *J. Phys. Oceanogr.*, *35*(12), 2337–2351, doi:10.1175/JPO2837.1.

Jerlov, N. G. (1976), *Marine Optics*, 231 pp., Elsevier, Amsterdam.

Killworth, P. D. (1996), Time interpolation of forcing fields in ocean models, *J. Phys. Oceanogr.*, *26*, 136–143, doi:10.1175/1520-0485(1996)026<0136:TIOFFI>2.0.CO;2.

Kondo, J. (1975), Air-sea bulk transfer coefficients in diabatic conditions, *Boundary Layer Meteorol.*, *9*, 91–112, doi:10.1007/BF00232256.

Kundu, P. K. (1990), *Fluid Mechanics*, 638 pp., Academic, New York.

Kuzmić, M. (1991), Exploring the effects of bura over the northern Adriatic: CZCS imagery and a mathematical model prediction, *Int. J. Remote Sens.*, *12*, 207–214, doi:10.1080/01431169108929646.

Kuzmić, M., M. Orlić, M. Karabeg, and L. Jeftić (1985), An investigation of wind-driven topographically controlled motions in the northern Adriatic, *Estuarine Coastal Shelf Sci.*, *21*, 481–499, doi:10.1016/0272-7714(85)90052-6.

Legates, D. R., and C. J. Wilmott (1990), Mean seasonal and spatial variability in a gauge corrected global precipitation, *Int. J. Climatol.*, *10*, 111–127, doi:10.1002/joc.3370100202.

Malačič, V. (1991), Estimation of the vertical eddy diffusion coefficient of heat in the Gulf of Trieste (northern Adriatic), *Oceanol. Acta*, *14*(1), 23–32.

Malačič, V., and B. Petelin (2001), Gulf of Trieste, in *Physical Oceanography of the Adriatic Sea, Past, Present and Future*, edited by B. Cushman-Roisin et al., pp. 167–177, Kluwer Acad., Dordrecht, Netherlands.

Malačič, V., and B. Petelin (2006), Numerical modeling of the winter circulation of the Gulf of Trieste (northern Adriatic), *Acta Adriat.*, *47*, 207–217.

Malačič, V., M. Celio, B. Čermelj, A. Bussani, and C. Comici (2006), Interannual evolution of seasonal thermohaline properties in the Gulf of Trieste (northern Adriatic) 1991–2003, *J. Geophys. Res.*, *111*, C08009, doi:10.1029/2005JC003267.

Marsaleix, P., C. Estournel, V. Kondrachoff, and R. Vehil (1998), A numerical study of the formation of the Rhône River plume, *J. Mar. Syst.*, *14*, 99–115, doi:10.1016/S0924-7963(97)00011-0.

Mellor, G. L. (2003), *Users gGuide for a Three-Dimensional, Primitive Equation, Numerical Ocean Model (June 2003 Version)*, 53 pp., Princeton Univ., Princeton, N. J.

Mellor, G. L., and T. Yamada (1982), Development of turbulence closure model for geophysical fluid problems, *Rev. Geophys.*, *20*, 851–875, doi:10.1029/RG020i004p00851.

Mosetti, F. (1967), Temperatura e salinitá nel Golfo di Trieste (risultati di un anno di determinazioni), *Adriatico*, *14*(5–6), 11–16.

Orlić, M., M. Kuzmić, and Z. Vučak (1986), Wind-curl currents in the northern Adriatic and formulation of botom friction, *Oceanol. Acta*, *9*(4), 425–431.

Paklar, G. B., V. Isakov, D. Koračin, V. Kourafalou, and M. Orlić (2001), A case study of bora-driven flow and density changes on the Adriatic shelf (January 1987), *Cont. Shelf Res.*, *21*, 1751–1783, doi:10.1016/S0278-4343(01)00029-2.

Pullen, J., J. D. Doyle, R. Hodur, A. Ogston, J. W. Book, H. Perkins, and R. Signell (2003), Coupled ocean-atmosphere nested modeling of the Adriatic Sea during winter and spring 2001, *J. Geophys. Res.*, *108*(C10), 3320, doi:10.1029/2003JC001780.

Pullen, J., J. D. Doyle, T. Haack, C. Dorman, and R. Signell (2007), Bora event variability and the role of air-sea feedback, *J. Geophys. Res.*, *112*, C03S18, doi:10.1029/2006JC003726.

Querin, S., A. Crise, D. Deponte, and C. Solidoro (2007), Numerical study of the role of wind forcing and freshwater buoyancy input on the circulation in a shallow embayment (Gulf of Trieste Northern Adriatic Sea), *J. Geophys. Res.*, *112*, C03S16, doi:10.1029/2006JC003611.

Raicich, F. (1994), Note on the flow rates of the Adriatic rivers, report, p. 8, Inst. Sper. Talassografico, Trieste, Italy.

Raicich, F. (1996), On the fresh water balance of the Adriatic Sea, *J. Mar. Syst.*, *9*, 305–319, doi:10.1016/S0924-7963(96)00042-5.

Reed, R. K. (1977), On estimating insolation over the ocean, *J. Phys. Oceanogr.*, *1*, 854–871.

Sanay, R., and A. Valle-Levinson (2005), Wind-induced circulation in semi-enclosed homogeneous, rotating basins, *J. Phys. Oceanogr.*, *35*(12), 2520–2531, doi:10.1175/JPO2831.1.

Smagorinsky, J. (1993), Some historical remarks on the use of nonlinear viscosities, in *Large Eddy Simulation of Complex Engineering and Geophysical Flows*, edited by B. Galperin and S. A. Orszag, pp. 3–36, Cambridge Univ. Press, Cambridge, U. K.

Stravisi, F. (1983), Some characteristics of the circulation in the Gulf of Trieste, *Thalassia Jugoslavica*, *19*(1–4), 355–363.

Stravisi, F., G. Pieri, and P. Berger (1981), Golfo di Trieste: Risultati delle misure correntometriche 1951–1954, *Bol. Soc. Adriatica Sci.*, *65*, 23–35.

Supić, N., and M. Orlić (1999), Seasonal and interannual variability of the northern Adriatic surface fluxes, *J. Mar. Syst.*, *20*, 205–229, doi:10.1016/S0924-7963(98)00083-9.

Supić, N., and I. Vilibić (2006), Dense water characteristics in the northern Adriatic in the 1967–2000 interval with respect to surface fluxes and Po river discharge rates, *Estuarine Coastal Shelf Sci.*, *66*(3–4), 580–593, doi:10.1016/j.ecss.2005.11.003.

Supić, N., M. Orlić, and D. Degobbis (2000), Istrian coastal countercurent and its year-to-year variability, *Estuarine Coastal Shelf Sci.*, *51*, 385–397, doi:10.1006/ecss.2000.0681.

Winant, C. D. (2004), Three-dimensional wind-driven flow in an elongated, rotating basin, *J. Phys. Oceanogr.*, *34*, 462–476, doi:10.1175/1520-0485(2004)034<0462:TWFIAE>2.0.CO;2.

Zavatarelli, M., and N. Pinardi (2003), The Adriatic Sea modelling system: A nested approach, *Ann. Geophys.*, *21*, 345–364.

Zavatarelli, M., N. Pinardi, V. H. Kourafalou, and A. Maggiore (2002), Diagnostic and prognostic model studies of the Adriatic Sea general circulation: Seasonal variability, *J. Geophys. Res.*, *107*(C1), 3004, doi:10.1029/2000JC000210.

V. Malačič and B. Petelin, Marine Biology Station, National Institute of Biology, Fornace 41, 6330 Piran, Slovenia. (vlado.malacic@mbss.org)